Journal of Southeast University (English Edition) Vol. 25, No. 4, pp. 496 – 500 Dec. 2009 ISSN 1003—7985

Voltage property analysis of piezoelectric floating mass actuator used in middle ear implant

Liu Houguang Ta Na Rao Zhushi

(State Key Laboratory of Mechanical System and Vibrations, Shanghai Jiaotong University, Shanghai 200240, China)

Abstract: Aiming at a kind of middle ear implant (MEI), the driving voltage of a piezoelectric floating mass actuator is analyzed using a 0.7Pb(Mg1/3Nb2/3)O3-0.3PbTiO3 (PMN-30% PT) stack as a new type of vibrator. For the purpose of facilitating the analysis, a simplified coupling model of the ossicular chain and the piezoelectric actuator is constructed. First, a finite element model of a human middle ear is constructed by reverse engineering technology, and the validity of this model is confirmed by comparing the simulated motion of the stapes footplate obtained by this model with experimental measurements. Then the displacement impedance of the incus long process is analyzed, and a single mass-spring-damper equivalent model of the ossicular chain attached with the clamp is derived. Finally, a simplified coupling model of the ossicular chain and the piezoelectric actuator is established and used to analyze the driving voltage property of the actuator. The results show that the required driving voltage decreases with the increase in the frequency, and the maximum required driving voltage is 20.9 V in the voice frequencies. However, in the mid-high frequencies where most sensorineural hearing loss occurs, the maximum required driving voltage is 3.8 V, which meets the low-voltage and low-power requirements of the MEI.

Key words: middle ear implant; piezoelectric actuator; floating mass; driving voltage

Hearing impairment is one of the most common diseases in our society. According to *the Second China National Sample Survey Data on Disability*, there are about 27 million people with hearing impairment in China[1]. Worldwide, the number is estimated to be more than 500 million. With the development of ear surgery, most of the conductive hearing loss can benefit from operation. However, there is still lack of effective treatment to sensorineural hearing loss. The majority of these hearing-impaired individuals can only turn to conventional hearing aids. However, conventional hearing aids have several inherent disadvantages, such as sound distortion, limited amplification, noise and ringing, discomfort, and cosmetic appearance[2]. For this reason, alternative methods to conventional hearing aids have been developed to overcome those limitations. Middle ear implant (MEI) is one of these alternative treatments.

Several different types of MEI are currently under development. Among them, the floating mass transducer (FMT) type, whose actuator is directly clamped to the ossicles, is widely utilized for its advantage of easy surgical operation[3-4]. Such type of MEI can still be classified into an electromagnetic one and a piezoelectric one in terms of its actuator's driving method. Until now, several kinds of the electromagnetic floating mass type MEI have been invented and undergone clinical trials, such as SOUNDTEC[3] and Soundbridge[4], but investigations of the piezoelectric floating mass type MEI are rarely reported. Considering that piezoelectric actuators have demonstrated many advantages including ease of fabrication, wider bandwidth, lower power consumption and more compatibility with external magnetic environments, Hong et al.[5] proposed a new type of piezoelectric MEI with a floating mass actuator. However, the middle ear's biomechanics was not considered in their research.

In this paper, we construct a simplified coupling mechanics model of the ossicular chain and the piezoelectric actuator, and use this model to investigate the driving voltage property of this new type of piezoelectric MEI.

1 Structure of Piezoelectric Floating Mass Type MEI

Fig. 1 shows the position where the piezoelectric actuator is implanted in the ossicular chain and an overall schematic of the piezoelectric floating mass type MEI. This MEI includes a microphone for receiving an acoustic signal from outside, a signal processing circuit for receiving the acoustic signal from the microphone to generate an acoustic electric signal, and a piezoelectric type actuator for generating an acoustic vibration signal in response to the acoustic electrical signal from the signal processing circuit.

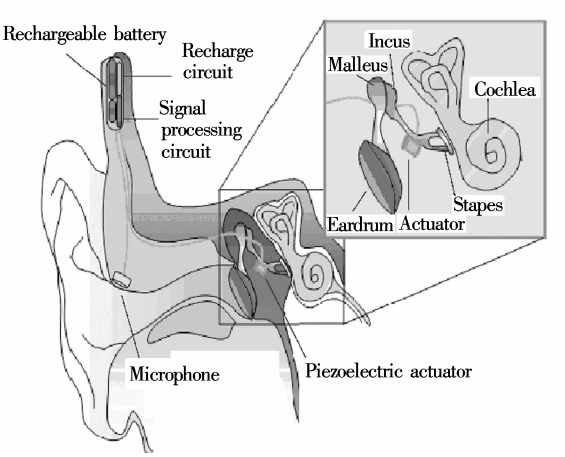

Fig. 1 Schematic of MEI system

Fig. 2 shows a schematic of the designed piezoelectric floating mass type actuator. This actuator consisting of a metal case, a clamp and a multi-layered piezoelectric stack,

Received 2009-03-16.

Biographies: Liu Houguang (1982—), male, graduate; Rao Zhushi (corresponding author), male, doctor, professor, zsrao@sjtu.edu.cn.

Foundation items: The National Natural Science Foundation of China (No. 10772121), the Med-Science Cross Research Foundation of Shanghai Jiaotong University (No. YG2007MS14).

Citation: Liu Houguang, Ta Na, Rao Zhushi. Voltage property analysis of piezoelectric floating mass actuator used in middle ear implant[J]. Journal of Southeast University (English Edition), 2009, 25(4): 496 – 500.

as shown in Fig. 2, is attached to the incus long process by its clamp. One side of the piezo-electric stack is fixed to the metal case, while the other side is stuck to the clamp. Then, the ossicle is vibrated by the repetition of the piezo-electric stack's expansion and contraction according to the applied voltage.

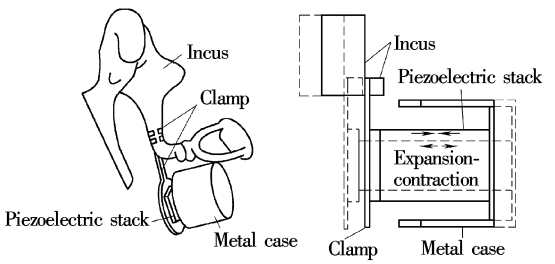

Fig. 2 Configuration of the floating mass type piezoelectric actuator

2 Coupling Mechanics Model of Middle Ear System and Piezoelectric Actuator

2.1 Middle-ear finite element model

To obtain the displacement impedance of the incus long process, we first construct a middle-ear finite element(FE) model with an actuator clamped as shown in Fig. 3. This finite element model is established based on a complete set of computerized tomography section images of a healthy volunteer's left ear by reverse engineering technology. The material properties and boundaries of this model are listed in Tab. 1 and Tab. 2. These material property values in Tab. 1 are taken from Refs. [6 −7], and the boundary conditions in Tab. 2 are taken from Refs. [8 −9]. Besides, the Poisson ratio is assumed to be 0.3 for all materials of the middle ear system, and the damping parameters are assumed to be $\alpha = 0\ s^{-1}$, $\beta = 0.1$ ms.

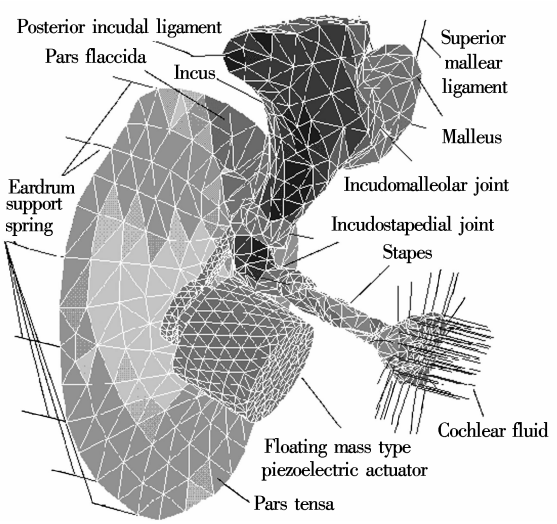

Fig. 3 The coupling model of the middle ear and the floating mass type piezoelectric actuator

In an attempt to confirm that our finite element model can give satisfactory predictions, comparisons against two experimental studies are made.

With a uniform harmonic pressure stimulus of 90 dB SPL applied to the lateral side of the eardrum in the FE model,

Tab. 1 Material properties of ear components

Ear components	Density $\rho/(10^3\,kg\cdot m^{-3})$	Young's modulus $E/(MN\cdot m^{-2})$
Pars tensor	1.20	32.0
Pars flaccida	1.20	10.0
Malleus head	2.55	1.41×10^4
Malleus neck	4.53	1.41×10^4
Malleus handle	3.70	1.41×10^4
Incudomalleolar joint	3.20	1.41×10^4
Incus body	2.36	1.41×10^4
Incus short process	2.26	1.41×10^4
Incus long process	5.08	1.41×10^4
Incudostapedial joint	1.20	0.6
Stapes	2.20	1.41×10^4

Tab. 2 Boundary conditions of the middle-ear FE model

Ear components	Stiffness $K/(kN\cdot m^{-1})$	Damping $C/(N\cdot s\cdot m^{-1})$
Superior mallear ligament	0.50	0
Anterior mallear ligament	0.30	0
Lateral mallear ligament	0.40	0
Posterior incudal ligament	0.50	0
Posterior stapedial muscle	0.05	0
Eardrum support spring	100	0
Tensor tympani tendon	0.04	0
Cochlear fluid	0.06	0.054

harmonic analysis is conducted across the frequency range of 0.25 to 10 kHz using ANSYS. The stapes footplate displacements are calculated and plotted with Gan et al.'s experimental data[10] as shown in Fig. 4. It shows that our FE model curve is lower than the mean experimental curve, especially in the frequencies above 750 Hz. However, the trend is similar to the mean experimental curve. The difference between the FE model prediction results and experimental data may come from the variations of individual temporal bones. Meanwhile, the stapes footplate velocity transfer functions(STF) are calculated and plotted with Aibara et al.'s experimental data[11] as shown in Fig. 5. Likewise, our FE model curve is close to the lower limits of the experimental curves, and consistent with the case of the footplate displacement in comparison with Gan et al.'s results.

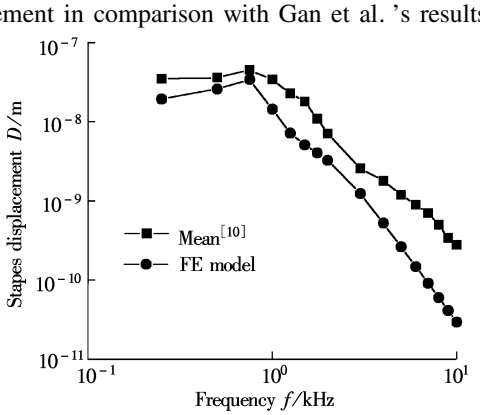

Fig. 4 Comparison between stapes footplate displacements predicted by the FE model and the experimental data

These comparisons show that our middle-ear FE model's predictions, in general, match experimental results obtained from human temporal bones. This middle-ear FE model can predict biomechanical characteristics of the human middle

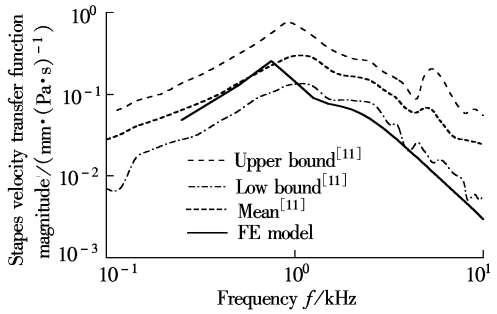

Fig. 5 Comparison of the stapes footplate velocity transfer function between the FE model prediction result and the experimental data

ear system.

2.2 Simplified coupling model of ossicular chain and piezoelectric actuator

Excessive amount of sound pressure can cause sensory nerve pain, so researchers often use 100 dB as their MEI's maximum amplified sound level[5]. But, the required force for driving the incus to the equivalent sound pressure of 100 dB SPL is unknown. Thus, in this simulation we select 100 dB SPL stimuli at the tempanic membrane as a reference. Fig. 6 shows the calculation results. Given that sensorineural hearing loss is usually very severe in high frequencies, the force required to drive the incus to the equivalent of 100 dB SPL is about 8.9 μN. This is consistent with the early experimental report[12]. Under this force's stimulation, the displacement of the incus long process where the actuator is clamped is also calculated as shown in Fig. 6. With these incus long process displacement data, the displacement impedance of the incus long process is derived. For conveniently constructing the simplified coupling model of the ossicular chain and the piezoelectric actuator, the system of the ossicular chain and the clamp is approximated to a mass-spring-damper model (the left part in Fig. 7). The equivalent mass m_i is presumed to be 27 mg, considering the mass of the incus. The equivalent damp c_i and stiffness k_i are derived from the above calculated displacement impedance of the incus long process.

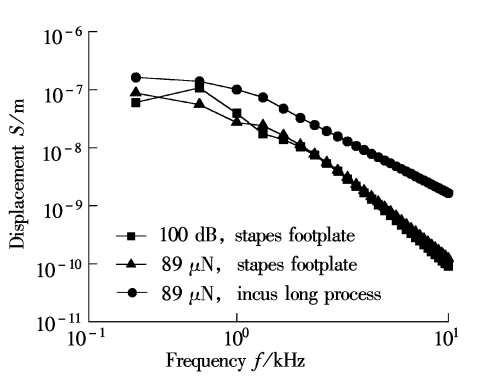

Fig. 6 Displacement of ossicular chain with eardrum stimulation and incus stimulation

According to the above analyses, our simplified coupling model of the ossicular chain and the piezoelectric actuator is established as shown in Fig. 7, where m_i, c_i and k_i stand for the equivalent mass, the equivalent damp and the equivalent

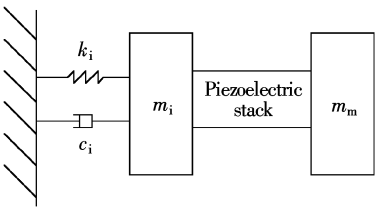

Fig. 7 Simplified coupling model of piezoelectric actuator and ossicular chain

stiffness of the ossicular chain, respectively. Besides, m_m stands for the mass of the metal case.

Fig. 8 presents the mechanical model of this coupling system. From the mechanical model, the equation of the motion of the coupling system can be derived as follows[13]:

$$\left.\begin{aligned} m_i\ddot{x}_i &= F_p - k_i x_i - c_i\dot{x}_i \\ m_m\ddot{x}_m &= F_p \end{aligned}\right\} \tag{1}$$

where F_p is the force applied to the piezoelectric stack.

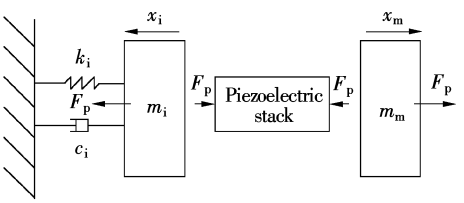

Fig. 8 Mechanical model of the coupling system of piezoelectric actuator and ossicular chain

The electromechanical behavior of the piezoelectric stack can be expressed as follows[13-14]:

$$\left.\begin{aligned} S_3 &= s_{33}^{E} T_3 + d_{33} E_3 \\ D_3 &= d_{33} T_3 + \varepsilon_{33}^{T} E_3 \end{aligned}\right\} \tag{2}$$

where $S_3 = \dfrac{\mathrm{d}l}{l} = \dfrac{x_i + x_m}{t_p n}$; S_3 and s_{33} are the axial stain and the elastic modulus of the piezoelectric material, respectively. $T_3 = -F_p/A$ is the axial stress applied to the piezoelectric material. A is the cross-sectional area of the piezoelectric stack and n is the number of layers in the piezoelectric stack. d_{33} is piezoelectric constant of the piezoelectric material. $E_3 = V_{in}/t_p$; D_3 and E_3 are the electric displacement and electric field strength, respectively. V_{in} is the driving voltage and t_p is the thickness of each layer in the piezoelectric stack.

Together with the expressions of T_3 and E_3, F_p can be expressed as

$$F_p = \frac{Ad_{33}}{s_{33}}E_3 - \frac{A}{s_{33}}S_3 = \frac{Ad_{33}}{t_p s_{33}}V_{in} - \frac{A}{s_{33}}\frac{x_i + x_m}{t_p n} = K_v V_{in} - K_e(x_i + x_m) \tag{3}$$

where $K_v = Ad_{33}/(t_p s_{33})$, $K_e = K_v/nd_{33}$.

Combining Eqs. (1) and (3) yields

$$\left.\begin{aligned} m_i\ddot{x}_i + K_e(x_i + x_m) &= K_v V_{in} - k_i x_i - c_i\dot{x}_i \\ m_m\ddot{x}_m + K_e(x_i + x_m) &= K_v V_{in} \end{aligned}\right\} \tag{4}$$

3 Driving Voltage of Piezoelectric Actuator

In our study, the piezoelectric stack has a cross-section of

1 mm × 1 mm and consists of 20 layers of crystal, each of 0.1 mm thickness, giving a depth of 2 mm. This piezoelectric stack is made up of PMN-30% PT piezoelectric material considering its vibration efficiency better than PZT materials. With 89 μN output force of the piezoelectric stack, the displacements of the incus, the metal case and the piezoelectric stack are derived from Eqs. (3) and (4) as shown in Fig. 9. Besides, the corresponding driving voltage is shown in Fig. 10.

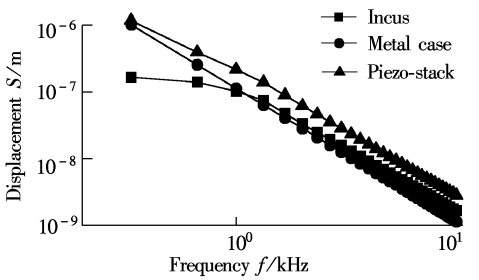

Fig. 9 Displacement of incus, metal case and piezoelectric stack under 89 μN stimulation force of piezoelectric stack

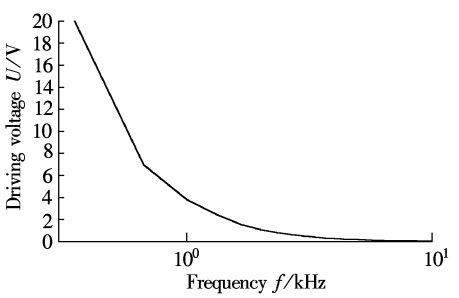

Fig. 10 The required driving voltage of piezoelectric actuator

Fig. 10 shows that, to stimulate the stapes footplate displacement equivalent to that from acoustic stimulation at 100 dB SPL, the required maximum driving voltage of the piezoelectric stack is 20.9 V in the voice frequency domain (0.3 to 3.4 kHz). In addition, the required driving voltage decreases with the increase in the frequency. Given that hearing impaired individuals often suffer from sensorineural hearing loss in a mid-high frequency range from about 1 to 4 kHz, the maximum required driving voltage of this piezoelectric stack is 3.8 V, which meets the safety requirements of the MEI.

4 Conclusions

To study the driving voltage property of a piezoelectric actuator of the middle ear implant, a simplified coupling model of the ossicular chain and the piezoelectric actuator is established. From the investigation, the following conclusions can be made:

1) The required driving voltage of the MEI's piezoelectric stack decreases with the increase in the frequency.

2) To stimulate the stapes footplate displacement equivalent to that from acoustic stimulation at 100 dB SPL, the required maximum driving voltage of the piezoelectric stack is 20.9 V in the voice frequency domain(0.3 to 3.4 kHz).

3) The maximum required driving voltage is 3.8 V in mid-high frequencies (> 1 kHz) where most sensorineural hearing losses occur.

Acknowledgement We are thankful to Dr S. K. Yin and Dr Z. N. Chen of Department of Otolaryngology of Shanghai Sixth People's Hospital, China, for the given facilities and encouragement.

References

[1] The Second China National Sample Survey Office on Disability. *The second China national sample survey data on disability* [M]. Beijing: China Statistics Press, 2007. (in Chinese)

[2] Meister H, Lausberg I, Kiessling J, et al. Determining the importance of fundamental hearing aid attributes [J]. *Otology & Neurotology*, 2002, **23**(4): 457 − 462.

[3] Silverstein H, Atkins J, Thompson J H Jr, et al. Experience with the SOUNDTEC implantable hearing aid [J]. *Otology & Neurotology*, 2005, **26**(2): 211 − 217.

[4] Truy E, Philibert B, Vesson J F, et al. Vibrant soundbridge versus conventional hearing aid in sensorineural high-frequency hearing loss: a prospective study [J]. *Otology & Neurotology*, 2008, **29**(5): 684 − 687.

[5] Hong E P, Kim M K, Park I Y, et al. Vibration modeling and design of piezoelectric floating mass transducer for implantable middle ear hearing devices [J]. *IEICE Trans Fundamentals*, 2007, **E90-A**(8): 1620 − 1627.

[6] Sun Q, Chang K H, Dormer K J, et al. An advanced computer-aided geometric modeling and fabrication method for human middle ear [J]. *Med Eng Phys*, 2002, **24**(9): 595 − 605.

[7] Beer H J, Bornitz M, Hardtke H J, et al. Modeling of components of the human middle ear and simulation of their dynamic behavior [J]. *Audiol Neurootol*, 1999, **4**(3/4): 156 − 162.

[8] Sun Q. Computer-integrated finite element modeling and simulation of human middle ear [D]. Oklahoma: The University of Oklahoma, 2001.

[9] Prendergast P J, Ferris P, Rice H J, et al. Vibro-acoustic modelling of the outer and middle ear using the finite-element method [J]. *Audiol Neurootol*, 1999, **4**(3/4): 185 − 191.

[10] Gan R Z, Dyer R K, Wood M W, et al. Mass loading on ossicles and middle ear function [J]. *Ann Otol Rhinol Laryngol*, 2001, **110**(5): 478 − 485.

[11] Aibara R, Welsh J T, Puria S, et al. Human middle ear sound transfer function and cochlear input impedance [J]. *Hearing Res*, 2001, **152**(1/2): 100 − 109.

[12] Ko W, Zhu W, Maniglia A. Engineering principles of mechanical stimulation of the middle ear [J]. *Otolaryngologic Clinics of North America*, 1995, **28**(1): 29 − 41.

[13] Liu H, Yan G Z, Ding G Q. Research on inertial piezoelectric actuator [J]. *Piezoelectric & Acoustooptics*, 2001, **23**(4): 275 − 278. (in Chinese)

[14] Choi S B, Hong S R, Han Y M. Dynamic characteristics of inertial actuator featuring piezoelectric materials: experimental verification [J]. *Journal of Sound and Vibration*, 2007, **302**(4/5): 1048 − 1056.

中耳植入式助听装置压电悬浮振子的电压特性分析

刘后广　塔　娜　饶柱石

（上海交通大学机械系统与振动国家重点实验室，上海 200240）

摘要：针对一种新型悬浮振子式中耳植入助听装置，分析了其振子的驱动电压特性，该振子由 0.7Pb（Mg1/3Nb2/3）O3-0.3PbTiO3（PMN-30%）叠堆实现. 为了辅助分析，建立了听骨链与振子的简化耦合力学模型. 首先利用逆向成型技术建立了人体中耳有限元模型，其可靠性通过镫骨底板的位移模拟值与实验测得数据对比得以验证；然后利用该中耳有限元模型分析了振子绑定装置处的位移阻抗特性，并基于此建立听骨链与绑定装置的等效力学模型；最后建立了听骨链与压电悬浮振子的耦合力学模型，分析了该振子的驱动电压特性. 研究结果表明:振子所需驱动电压随着频率的增大而减小；在语音频段，所需的最大驱动电压为 20.9 V；在感音神经性听力损伤多发生的中高频段，该驱动电压不高于 3.8 V，满足中耳植入式助听装置低电压、低能耗的要求.

关键词：中耳植入式助听装置；压电振子；悬浮质量；驱动电压

中图分类号：TN384